Insight into the Mechanism of Phosphoenolpyruvate Mutase Catalysis Derived from Site-Directed Mutagenesis Studies of Active Site Residues†

Yong Jia,‡ Zhibing Lu,‡ Kui Huang,§ Osnat Herzberg,§ and Debra Dunaway-Mariano*,‡

Department of Chemistry, University of New Mexico, Albuquerque, New Mexico 87131, Department of Chemistry and Biochemistry, University of Maryland, College Park, Maryland 20742, and Center for Advanced Research in Biotechnology, University of Maryland Biotechnology Institute, 9600 Gudelsky Drive, Rockville, Maryland 20850

Received April 2, 1999; Revised Manuscript Received July 8, 1999

ABSTRACT: PEP mutase catalyzes the conversion of phosphoenolpyruvate (PEP) to phosphonopyruvate in biosynthetic pathways leading to phosphonate secondary metabolites. A recent X-ray structure [Huang, K., Li, Z., Jia, Y., Dunaway-Mariano, D., and Herzberg, O. (1999) *Structure* (in press)] of the *Mytilus edulis* enzyme complexed with the Mg(II) cofactor and oxalate inhibitor reveals an α/β-barrel backbone-fold housing an active site in which Mg(II) is bound by the two carboxylate groups of the oxalate ligand and the side chain of D85 and, via bridging water molecules, by the side chains of D58, D85, D87, and E114. The oxalate ligand, in turn, interacts with the side chains of R159, W44, and S46 and the backbone amide NHs of G47 and L48. Modeling studies identified two feasible PEP binding modes: model A in which PEP replaces oxalate with its carboxylate group interacting with R159 and its phosphoryl group positioned close to D58 and Mg(II) shifting slightly from its original position in the crystal structure, and model B in which PEP replaces oxalate with its phosphoryl group interacting with R159 and Mg(II) retaining its original position. Site-directed mutagenesis studies of the key mutase active site residues (R159, D58, D85, D87, and E114) were carried out in order to evaluate the catalytic roles predicted by the two models. The observed retention of low catalytic activity in the mutants R159A, D85A, D87A, and E114A, coupled with the absence of detectable catalytic activity in D58A, was interpreted as evidence for model A in which D58 functions in nucleophilic catalysis (phosphoryl transfer), R159 functions in PEP carboxylate group binding, and the carboxylates of D85, D87 and E114 function in Mg(II) binding. These results also provide evidence against model B in which R159 serves to mediate the phosphoryl transfer. A catalytic motif, which could serve both the phosphoryl transfer and the C−C cleavage enzymes of the PEP mutase superfamily, is proposed.

Phosphoenolpyruvate mutase (PEP mutase)[1] catalyzes the conversion of PEP to phosphonopyruvate (Ppyr), the key P−C bond-forming step of the biosynthetic pathways leading to phosphonate natural products (*1*−*3*) (Scheme 1). Phosphonates are found in a wide range of organisms including humans, yet their synthesis has been demonstrated in only a few, wherein the phosphonate performs a highly specialized function (for a recent review see ref *4*). In some bacteria the phosphonate produced is excreted to serve in chemical warfare (*5*), in the cell membranes of some parasites phosphatase/lipase-resistant phosphonolipids function as a coat of armor allowing host inhabitation (*6*−*9*), and in certain marine organisms phosphonoglycosides appear to function in cell−cell signaling (*10, 11*).

It has been hypothesized that on primitive earth, and perhaps in early life forms, phosphonates preceded phosphates (*12, 13*). Because the P−C bond is intrinsically higher in energy than the P−O bond, as the earth's atmosphere became increasingly oxygenated, phosphates would replace phosphonates and the enzymes which catalyzed P−C bond formation and cleavage would be replaced by enzymes that specialize in P−O bond formation and cleavage. Thus, while the possibility that PEP mutase evolved after the decline of biological phosphonates cannot be dismissed, it is likely that this enzyme has persisted from the beginning of cellular metabolism.

Irrespective of whether PEP mutase is an ancient or relatively modern enzyme, the P−O to P−C bond transformation that it catalyzes is unique among enzyme-mediated reactions. There is only one other enzyme known to catalyze such a reaction (Scheme 1) and that is CPEP mutase (*14*), which functions along with the PEP mutase in the biosynthetic pathway leading to the natural phosphinate bialaphos (L-alanyl-L-alanyl-2-amino-4-(methylphosphinyl)butanoic acid).

† This work was supported by a grant from the National Institutes of Health (GM 28688 to D.D.-M.) and by a grant from the National Science Foundation (MCB9316934 to O.H.).

* Corresponding author. Tel: 505-277-3383. Fax: 505-277-6202. E-mail: dd39@unm.edu.

‡ University of New Mexico and University of Maryland.

§ University of Maryland Biotechnology Institute.

[1] Abbreviations: PEP, phosphoenolpyruvate; Ppyr, phosphonopyruvate; AEP, 2-aminoethylphosphonate; CPEP, carboxyphosphonoenolpyruvate; Pald, phosphonoacetaldehyde; BSA, bovine serum albumin; PMSF, phenylmethanesulfonyl fluoride; TEA, triethanolamine; ADP, adenosine 5′-diphosphate; EDTA, disodium ethylenediaminetetraacetate; SDS, sodium dodecyl sulfate; PAGE, polyacrylamide gel eletrophoresis; DTT, dithiothreitol; NADH, dihydronicotinamide adenine dinucleotide; HEPES, 4-(2-hydroxyethyl)-1-piperazineethanesulfonic acid; IPTG, isopropyl thio-β-galactoside; LB, Luria−Bertani; FPLC, fast-performance liquid chromatography; CD, circular dichroism.

10.1021/bi990771j CCC: $18.00
Published on Web 10/05/1999

Scheme 1

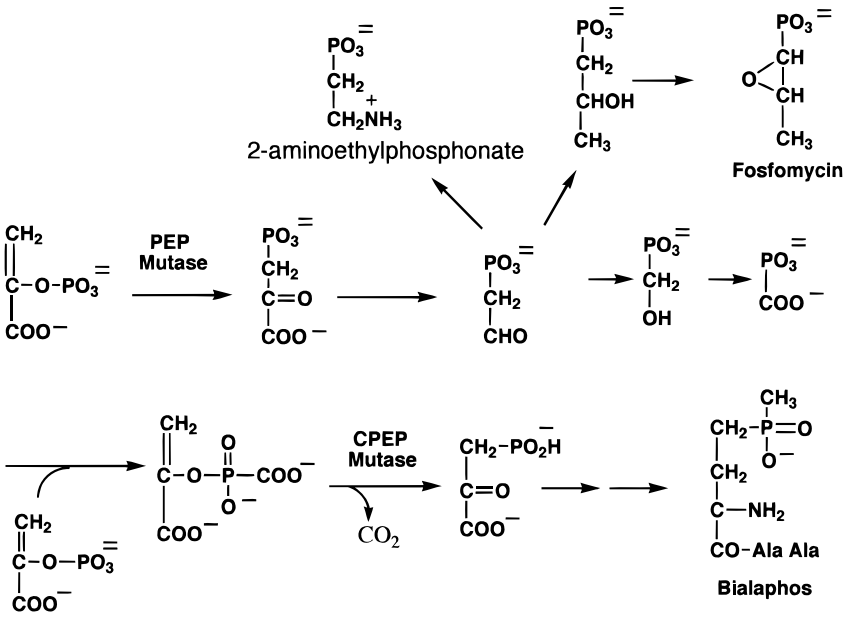

On the level of amino acid sequence, the two enzymes are homologous (*15*). The three-dimensional structure of CPEP mutase is not known, but that of *Mytilus edulis* PEP mutase bound to Mg(II) cofactor and oxalate inhibitor has been recently reported (*16*). As illustrated in Figure 1A, the PEP mutase monomer adopts an α/β-barrel fold in which one of the eight α-helices has peeled away from the β-barrel, thus allowing it to function in subunit−subunit binding within the functional homotetramer (shown in ref *16*). As with all other α/β-barrel enzymes examined to date, the active site region of the PEP mutase [identified in Figure 1A by Mg(II) and oxalate] is located at the C-terminal ends of the barrel strands. The topology of the active site (illustrated in Figure 1A by colored segments) is, however, unique among α/β-barrel enzymes including those that bind Mg(II)/PEP and/or Mg(II)/pyruvate (viz., pyruvate kinase, pyruvate phosphate dikinase, enolase, and *N*-acetylneuraminate lyase). Indeed, as will be described in this paper, PEP mutase along with CPEP mutase, isocitrate lyase, 2-methylisocitrate lyase, and several proteins of yet unidentified function forms a new α/β-barrel enzyme superfamily, represented by the active site fold shown in Figure 1A.

Our continuing interest in PEP mutase centers on the mechanism by which it catalyzes the transfer of the PEP phosphoryl group from the C(2) oxygen to C(3). Previous studies of the *Tetrahymena pyriformis* PEP mutase catalyzed reaction have shown that the phosphoryl transfer is intramolecular and that it occurs with retention of stereochemistry at phosphorus (*17, 18*). On the basis of these findings, two stepwise mechanisms may account for PEP mutase catalysis (Scheme 2). Specifically, the reaction may proceed through an associative, double-displacement pathway in which the enzyme transfers the phosphoryl group from the C(2) oxygen of PEP to an active site residue and, then, to the C(3) of the pyruvate enolate intermediate (mechanism I). The alternative mechanism involves dissociation of metaphosphate from the C(2) oxygen of PEP followed by bond formation to the C(3) of the pyruvate enolate intermediate (mechanism II). Attempts to verify one of these two mechanisms have, to date, been unsuccessful. Single-turnover experiments, designed to trap the pyruvate enolate intermediate (key to both pathways), have failed to do so (*19*), indicating that it does not accumulate to a detectable level on the enzyme during turnover.[2] Single-turnover experiments (*22*) designed to trap the putative phosphoenzyme intermediate formed via mechanism I of Scheme 2 have also been unsuccessful, indicating that such an enzyme species is not formed or that it cannot be easily detected.

At the outset of the present study, we examined the recently determined active site structure of the *M. edulis* PEP mutase (*16*) for possible clues regarding its catalytic mechanism. A close view of the PEP mutase active site, with Mg(II) and oxalate bound, is provided in Figure 1B. In this structure, Mg(II) is seen coordinated by the carboxylate of D85 and the two carboxylate substituents of the oxalate ligand. The three remaining coordination positions on the metal are filled by water ligands which, in turn, interact with the side chains of E114, D87, D58, and K120. In addition to coordinating to the metal ion, oxalate forms an ion pair with R159 and H-bonds with the side chains of S46 and Trp 44 and the backbone amide NHs of G47 and L48. These multiple binding interactions account for the tight binding observed between oxalate and PEP mutase (*20*).

The structure of the PEP mutase complex with Mg(II) and oxalate provides a clear view of the active site but leaves some uncertainty as to the exact positions that might be assumed by the metal ion and ligand in the enzyme−substrate complex. In one model (model A shown in Figure 2) the PEP ligand was docked close to but in a different orientation than the oxalate such that the carboxylate group interacts

[2] The only experimental evidence supporting the formation of a pyruvate enolate intermediate, common to both reaction pathways, is the 10-fold stronger binding of the oxalate ($K_i = 25$ μM vs Ppyr) over the substrate PEP ($K_i = 350$ μM vs Ppyr) (*20*). Previous studies have shown that enzymes which catalyze phosphoryl transfer from PEP (e.g., pyruvate kinase and pyruvate phosphate dikinase) bind oxalate much tighter than PEP or pyruvate (*21*). For these enzymes the preferential binding observed with oxalate has been attributed to its close resemblance to the putative reaction intermediate, pyruvate enolate. In analogy, the tight binding of oxalate to PEP mutase is consistent with the formation of a pyruvate enolate intermediate.

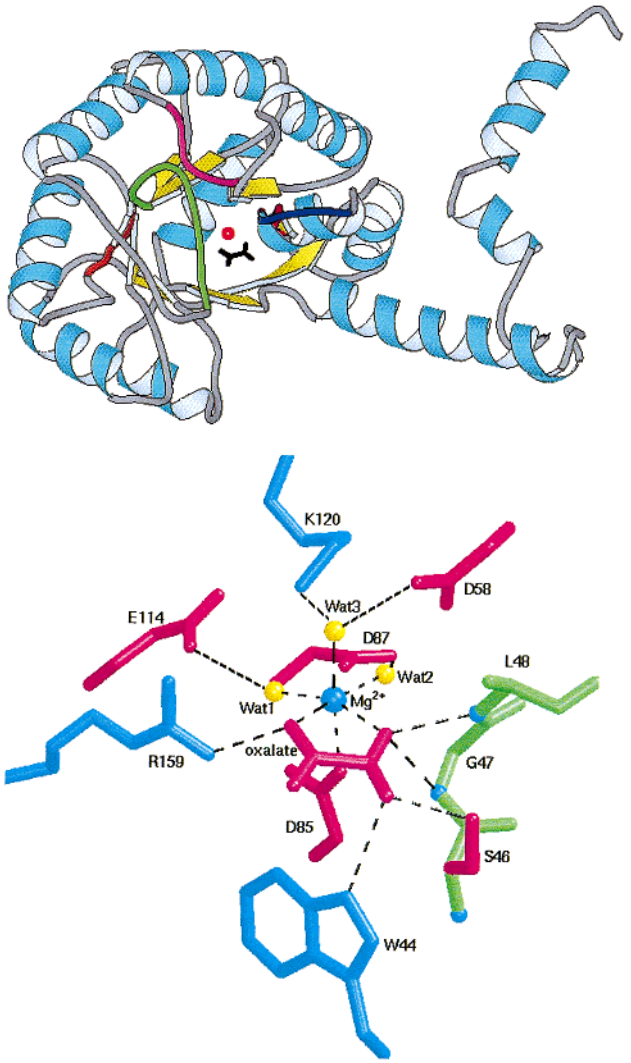

FIGURE 1: (A, top) *M. edulis* PEP mutase monomer with bound Mg(II) and oxalate as generated from the coordinates reported in ref *16* using Molscript (*54*) and Insight II. The PEP mutase catalytic residues are located on the C-terminal ends of barrel β-strands 2 (the oxyanion hole formed by residues 46−48 is shown in red; the sequence region 55−58 containing the putative active site nucleophile D58 is shown in blue), 3 [the sequence region 84−91 containing the Mg(II) binding residues D85 and D87 is shown in magenta], 4 [the sequence region 114−124 containing the Mg(II) binding residue E114 and the PEP phosphoryl group binding residue K120 is shown in green], and 5 (the sequence region 158−162 containing the PEP carboxylate binding residue R159 is shown in orange). The Mg(II) ion is represented in red and the oxalate ligand in black. (B, bottom) Active site residues involved in Mg(II) and oxalate binding.

with R159 and the phosphoryl group interacts with the side chain of K120 and backbone amide NH of L48. In this position, the PEP phosphoryl group (as well as the Ppyr phosphoryl group; see ref *16*) lies in close proximity to D58. The Mg(II) was shifted from its original location in the PEP mutase−Mg(II)−oxalate complex (Figure 1B), allowing it to coordinate to the carboxylate and C(2) oxygen of the PEP ligand[3] and form direct interactions with three of the four active site carboxylate residues: D85, D87, and E114. Model A predicts that D58 would serve in the well-precedented role

[3] Activation of PEP for phosphoryl transfer via bidentate Mg(II) coordination has been observed in pyruvate kinase (*23*) and pyruvate phosphate dikinase (*24*).

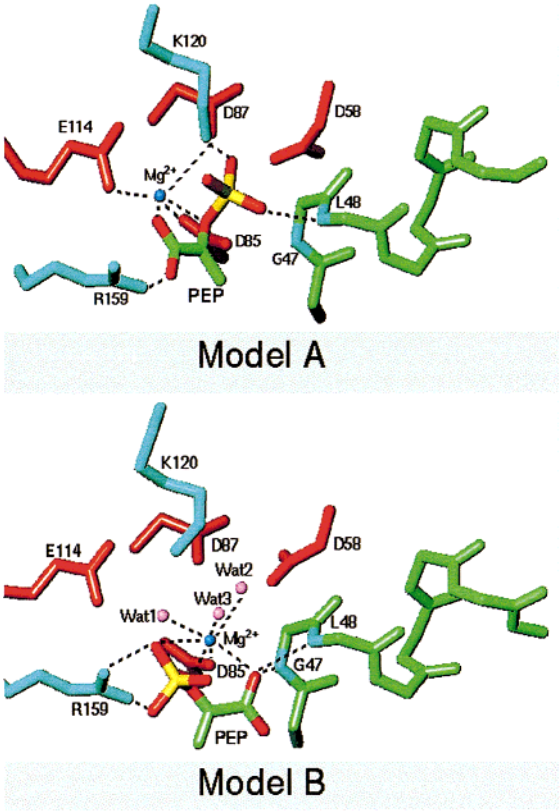

FIGURE 2: *M. edulis* PEP mutase active site derived from the X-ray crystal structure of the Mg(II)/oxalate complexed enzyme (*16*) into which PEP has been modeled in two different orientations (viz., models A and B). Possible electrostatic interactions are shown as broken lines. Because the Mg(II) position was altered in model A, the water ligands are not shown.

Scheme 2

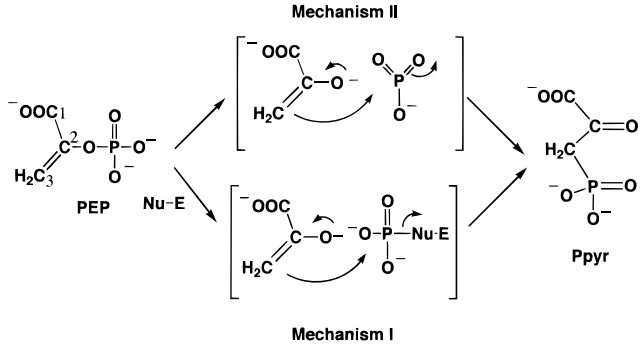

of active site nucleophile (*25*−*28*) and, therefore, would be essential to catalytic turnover. Thus, we set out to test this model by replacing D58 with alanine and determining whether residual catalytic activity exists in the mutant enzyme. Active site mutants bearing alanine substitutions at the D85, D87, and E114 sites were also examined.

An alternate model (model B of Figure 2) places the PEP in the oxalate position with the phosphoryl group interacting with R159 and the carboxylate substituent interacting with the backbone amide NHs of G47 and L48 and the side chains of S46 and W44. Mg(II) remains coordinated to the same groups observed in the crystal structure (Figure 1B). The utilization of an arginine side chain, as seen here, for binding and activating the phosphoryl group for transfer is commonplace among phosphoryl transfer enzymes (*29*). However, since there are no nucleophilic residues within reach

of the PEP phosphoryl moiety, it must be assumed that the R159 also functions as a temporary docking site for metaphosphate as it dissociates from the PEP (mechanism II of Scheme 2). Alternatively, in its unprotonated form, the R159 might serve as the active site nucleophile (as is required by mechanism I). In either role required by model B, the R159 would be essential to catalytic turnover, and thus, we set out to test model B by replacing this residue with alanine and determining whether residual catalytic activity exists in the mutant enzyme.

In this paper we describe the cloning, sequencing, expression, and mutagenesis of the *M. edulis* PEP mutase gene in *Escherichia coli*. The kinetic properties of the PEP mutase D58A, D85A, D87A, E114A, and R159A mutants support the active site model A (Figure 2) and the double-displacement mechanism of catalysis (mechanism I, Scheme 2). Tentative roles are assigned to the active site residues, and in recognition of their invariance within the PEP mutase superfamily, a general catalytic motif is proposed.

MATERIALS AND METHODS

PEP Mutase Gene Cloning and Sequencing. The *M. edulis* cDNA Uni-ZAP XR phage library (constructed by Stratagene) was screened on a lawn of XL1-Blue MRF′ host cells (Stratagene) using a ^{32}P-labeled 360 base pair fragment of the PEP mutase gene as the probe in Southern blot analysis (*30*). The gene fragment was obtained by PCR (*31*) amplification of cDNA prepared from *M. edulis* mRNA using the degenerate primers designed from the mussel PEP mutase N-terminal sequence (STKVKKTTQLKQMLN) and from the sequence of an internal V8 protease generated fragment (DKLFPKTNSLHDGRA) (*32*). The pBluescript phagemid was subjected to in vivo excision from the Uni-ZAP vector using ExAssist helper phage and SOLR cells (Stratagene), and then following plasmid purification, the full-length PEP mutase was sequenced using the dideoxynucleotide termination method (*33*). *Nde*I and *Bam*HI restriction sites were added to the ends of the gene using PCR techniques prior to ligation in the linearized pET3c vector (Stratagene). The ligation mixture was used to transform (*30*) competent BL21-(DE3) *E. coli* cells (Stratagene). The recombinant plasmid obtained from a positive clone was verified by gene sequencing and given the name YJ-102.

Expression and Purification of Recombinant M. edulis PEP Mutase. For enzyme purification, four 2 L cultures of YJ-102 *E. coli* cells (7 h at 30 °C; $OD_{600} = 0.8-1.0$; ca. 25 g cell total) were each induced by 4 h incubation with 8 mL of 100 mM IPTG. The harvested cells were resuspended in 250 mL of lysis buffer (50 mM K^+Hepes, pH 7.5, 5 mM DTT, 1 mM EDTA, 1 mM benzamide hydrochloride, 50 μg/mL trypsin inhibitor, 1 mM 1,10-phenanthroline, and 0.1 mM PMSF) and lysed by passing through a French pressure cell press at 1200 psi. The supernatant, obtained by centrifugation of the lysate at 15 000 rpm for 1 h, was chromatographed at 4 °C on a 4.7 × 50 cm DEAE-cellulose column with 250 mL of buffer A (50 mM TEA, pH 7.5, 0.5 mM DTT, and 5 mM $MgCl_2$) followed by a 2 L linear gradient of 0−0.2 M KCl in buffer A serving as eluant. The column fractions were assayed for PEP mutase activity using a coupled assay with pyruvate kinase and lactate dehydrogenase (*34*). The PEP mutase containing fractions (eluted at ca. 0.15 M KCl) were pooled and concentrated to 50 mL with an Amicon ultrafiltration apparatus (PM10) before being loaded onto a 2.8 × 25 cm hydroxyapatite column which had been preequilibrated with buffer A. The column was eluted with 25 mL of buffer A followed by an 1800 mL linear gradient of 0.05−0.5 M KH_2PO_4 in buffer A. The PEP mutase containing fractions (eluted at ca. 0.17 M KH_2PO_4) were pooled and concentrated to 12 mL before 4 mL aliquots were chromatographed on a 10 cm FPLC HR 5/5 Mono Q column which had been preequilibrated with buffer A. The column was eluted with 2 mL of 0.02 M KCl in buffer A, followed by a 30 mL linear gradient of 0.02−0.2 M KCl in buffer A. PEP mutase fractions (eluting at ca. 0.16 M KCl) were analyzed by SDS−PAGE.

Characterization of Recombinant PEP Mutase. (A) Molecular Size Determination. The recombinant PEP mutase subunit size was determined by SDS−PAGE analysis (12% separating gel, 3% stacking gel) using the 10 kDa ladder from BRL as the molecular weight standard. A linear semilog plot of log molecular weight vs distance traveled on the gel was constructed. The subunit size of the mussel PEP mutase was determined from the measured distance traveled on the gel by extrapolation from the plot. The molecular size of the recombinant PEP mutase was determined using gravity flow gel filtration techniques. The chromatography of the mutase was carried out on a 1.5 × 180 cm Sephacryl S-200 column (equilibrated with buffer A) that had been calibrated using the Pharmacia gel filtration calibration kit (thyroglobulin 669 000; catalase 232 000; albumin 67 000; chymotrypsinogen A 25 000) according to the manufacturer's instructions. The chromatography was carried out at 4 °C using 0.1 M KCl in buffer A as eluant and a peristaltic pump to maintain a constant flow rate of 0.5 mL/min. The plots of the elution volume of the molecular weight standards vs log molecular weight were found to be linear. The elution volume measured for mussel PEP mutase was used to extrapolate the molecular weight from the plot.

(B) Steady-State Kinetic Constant Determination. The k_{cat} and K_m values for recombinant PEP mutase were determined from initial velocity data. The rate of PEP formation in reactions containing ca. 0.002 unit/mL PEP mutase, 5 mM $MgCl_2$, varying concentrations of Ppyr (1−100 μM), 50 mM K^+Hepes (pH 7.5, 25 °C), and the coupling system (1 mM ADP, 0.2 mM NADH, 10 units/mL pyruvate kinase, and 10 units/mL lactate dehydrogenase) was monitored by measuring the decrease in solution absorbance at 340 nm ($\Delta\epsilon$ = 6.2 mM^{-1} cm^{-1}). The initial velocity data were analyzed using eq 1 and the FORTRAN HYPERL program of Cleland (*35*)

$$v_0 = V_m[S]/(K_m + [S]) \quad (1)$$

where v_0 = initial velocity, V_m = maximum velocity, [S] = substrate concentration, and the K_m = Michaelis constant for substrate. The k_{cat} value was calculated from V_m and [E] according to the equation $k_{cat} = V_m/[E]$, where [E] is the molar concentration of PEP mutase [based on the protein concentration determination using the Bradford (*36*) assay] used to catalyze the reactions.

(C) Circular Dichroism Spectral Determinations. CD spectra of wild-type and mutant PEP mutase [0.1 mg/mL in 50 mM TEA/5 mM Mg(II), pH 7.5] were measured at the

Table 1: Purification of the Mussel *M. Edulis* PEP Mutase from Crude Protein Isolated from the Supernatant of 25 g (7 L of Culture) of Lysed Cells

step	total protein[a] (mg)	total act.[b] (unit)	sp act. (units/mg)	yield (%)	purification (x-fold)
DEAE-cellulose	718	7854	10.9	100	1
hydroxapatite	117	5846	50.0	74	4.5
Mono Q	26	1705	65.5	21	6

[a] The protein concentration was monitored at 280 nm and estimated according to 1 OD_{280} = 1 mg/mL. [b] One unit of enzyme activity was defined as the amount of enzyme required for production of 1 mmol of PEP from Ppyr/min (measured using the pyruvate kinase/lactate dehydrogenase coupling assay under conditions of pH 7.5, $[Mg^{2+}]$ = 5 mM, [Ppyr] = 1 mM, and 25 °C as described in Materials and Methods).

Table 2: Yields and Kinetic Properties of the *M. Edulis* PEP Mutase Site-Directed Mutants

enzyme (μM)	yield (mg/g of cell)	k_{cat}[a] (s^{-1})	K_m, Ppyr (μM)	K_m, Mg(II)[b]
wild type	1.0	33.9 ± 0.4	1.59 ± 0.04	81 ± 3
D85A	0.3	0.072 ± 0.002	2500 ± 100	34 ± 3
D87A	4.0	0.171 ± 0.003	3.4 ± 0.2	40 ± 2
D58A	0.1	inactive[c]		
E114A	27.0	0.00377 ± 0.00008	116 ± 7	630 ± 40
R159A	11.0	0.0010 ± 0.00001	54 ± 2	

[a] The assay mixture contained 50 mM K^+Hepes (pH 7.5), 5 mM $MgCl_2$, 1 mM ADP, 0.2 mM NADH, 10 units/mL pyruvate kinase, 10 units/mL lactate dehydrogenase, and varying Ppyr concentration. [b] The assay mixture contained 50 mM K^+Hepes (pH 7.5), 1 mM Ppyr, and varying $MgCl_2$ concentration. [c] This value is below the activity detection limit, which is ca. 1×10^{-7} s^{-1}.

Protein and Carbohydrate Facility of the University of Michigan.

Preparation of PEP Mutase Mutants. Site-directed mutagenesis was carried out with the four-primer PCR technique and protocol described in ref *31* using plasmid YJ-102 as the template. Mutant plasmids isolated from JM109 *E. coli* host cells were subjected to DNA sequencing to verify the correct PEP mutase gene sequence and then used to transform BL21(BE3) *E. coli* cells for expression. The PEP mutase mutants were purified and characterized in the same manner as described above for the wild-type PEP mutase.

Identification of the PEP Mutase Superfamily. The four PEP mutase sequences were used to search available NCBI sequence databases using Advanced and PSI BLAST programs (*37*). The sequences that were found by more than two query sequences were assigned to the set of candidates of PEP mutase homologues. From this group, a divergent set of sequences was generated such that no sequence was more than 50% identical to any other sequence in the set. These sequences were aligned using ClustalW (*38*) provided by the Wisconsin Genetics Computer Group.

RESULTS

Recombinant M. edulis PEP Mutase. The *M. edulis* PEP mutase gene was isolated from a cDNA phage library and expressed in *E. coli* BL21(DE3) cells using the pET3c vector. The protocol used to purify the recombinant enzyme from this system [*Mytilus edulis* PEP mutase/*E. coli* BL21(DE3)], illustrated in Table 1, was designed after that used for the purification of the wild-type enzyme (*32*). The enzyme was obtained in pure form, as determined by SDS−PAGE analysis, in a yield of 1 mg/g of cell (SA = 66 units/mg at pH = 7.5, 25 °C).

The subunit size of the purified recombinant enzyme was determined using SDS−PAGE techniques to be 33.2 kDa, which compares favorably with the value of 34 kDa measured for the wild-type enzyme isolated from *M. edulis* tissue (*32*). The molecular weight of the native *M. edulis* PEP mutase, previously determined by gravity flow gel filtration chromatography to be 144 kDa, is consistent with a tetrameric subunit structure (*32*). In the present study, the molecular size of the recombinant enzyme was determined as 142 kDa. The steady-state kinetic constants determined (in the Ppyr to PEP reaction direction) at pH 7.5 and 25 °C for the PEP mutase isolated from the two sources are essentially equivalent: (Ppyr) $K_m = 1.56 \pm 0.04$ mM and $k_{cat} = 33.9 \pm 0.4$ s^{-1} for the recombinant enzyme (Table 2) vs (Ppyr) $K_m = 3.3 \pm 0.3$ mM and $k_{cat} = 34$ s^{-1} for the *M. edulis* enzyme (*32*). The CD spectrum of recombinant PEP mutase in 50 mM TEA/5 mM Mg(II) is characterized by a trough spanning 190−240 nm with a $\lambda_{max} = 217$ ($\theta = -2.93 \times 10^6$ deg·cm^2/dmol).

Sequence Determination of the M. edulis PEP Mutase Gene. The *M. edulis* PEP mutase gene (Accession Number 295644) encodes a protein of 295 amino acids having a calculated molecular mass of 32 912 Da and isoelectric p*I* of 5.51. In a previous study (*32*) the N-terminal sequence of the PEP mutase isolated from *M. edulis* tissue was determined to be STKVKKTTQLKQMLN, indicating that the N-terminal Met residue is removed posttranslationally. The sequence of an internal V8 protease peptide fragment was found to be DKLFPKTNSLHDGRA, corresponding to residues 115−129 shown in Figure 3. The alignment of the *M.edulis* PEP mutase sequence with those of the PEP mutase from *T. pyriformis* (*15*) (71% sequence identity), *Streptomyces hygroscopicus* (*39*) (43% sequence identity), and *Streptomyces wedmorensis* (*40*) (31% sequence identity) reveals that 21% of the residues are identical throughout all four sequences. Among these stringently conserved residues (colored magenta in Figure 3) are the active site residues pictured in Figure 1B: W44, S46, D58, D85, D87, E114, K120, and R159. The residues that form the oxyanion hole, G47 and L48, are also well conserved [L48 is invariant and G46 is replaced (by S) in only one out of the four sequences].

Preparation and Properties of PEP Mutase Site-Directed Mutants. The mutant genes were prepared by PCR using the YJ-102 plasmid as template and then inserted into the pET3c vector for expression in *E. coli* BL21(DE3). The yields of the purified mutant proteins are reported in Table 2 along with the steady-state kinetic values determined for catalysis of the reaction of Ppyr to PEP at 25 °C and pH 7.5 with Mg(II) serving as activator. D58A, D85A, D87A, E114A, and R159A PEP mutase retained a detectable level of catalytic activity but D58A PEP mutase did not. The CD spectrum of the D58A PEP mutase in 50 mM TEA/5 mM Mg(II), characterized by a trough spanning 190−240 nm with a $\lambda_{max} = 217$ ($\theta = -3.09 \times 10^6$ deg·cm^2/dmol), is essentially the same as that measured for wild-type PEP mutase. The stability and the chromatographic behavior of D58A are not noticeably different from those of the wild-type enzyme.

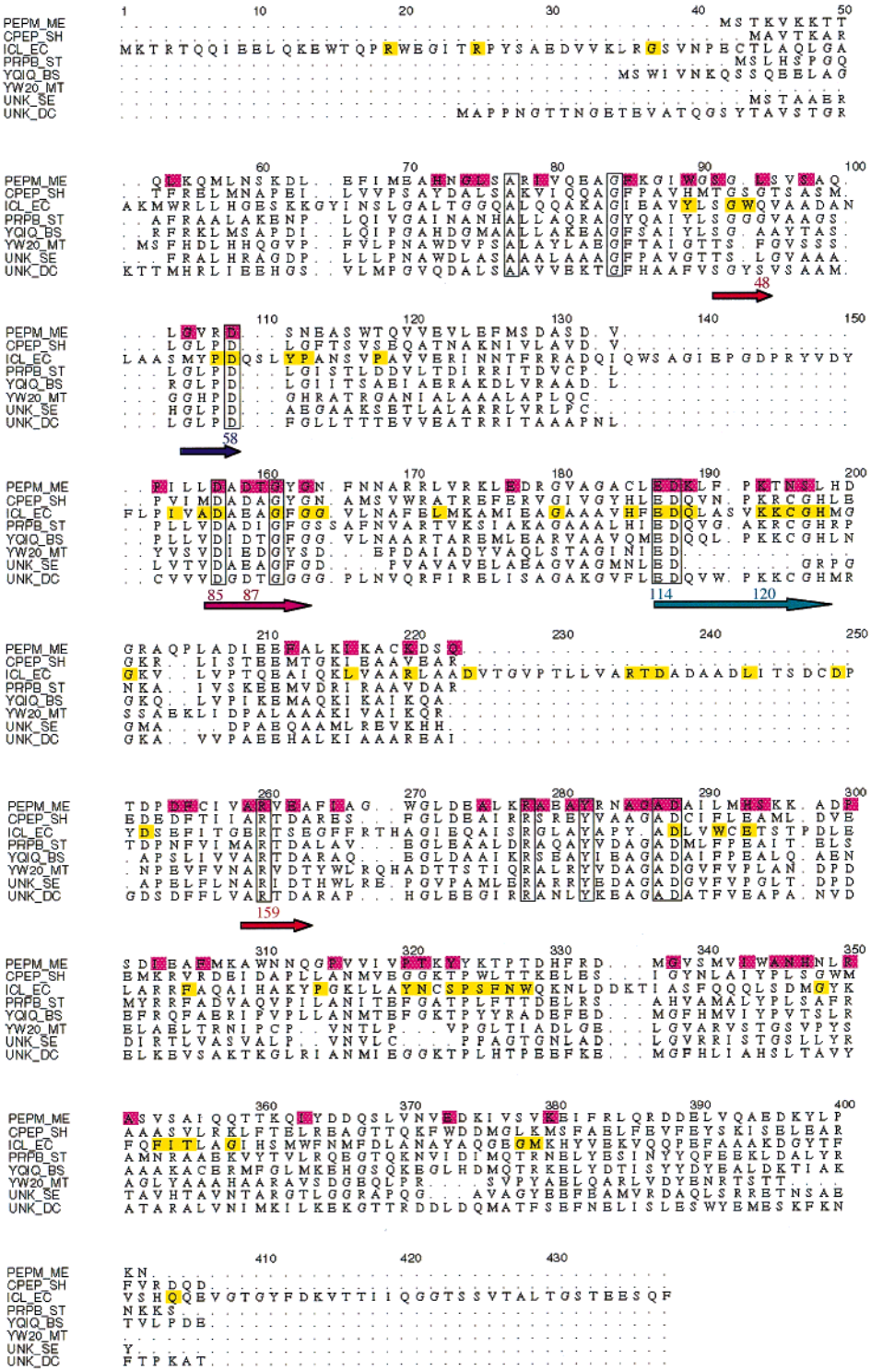

FIGURE 3: Alignment of the amino acid sequences of the PEP mutase structural homologues identified from Advanced BLAST and PSI BLAST (*37*) searches. The sequences shown are PEP mutase from *M. edulis* (PEPM_ME; Accession Number 295644), CPEP mutase from *S. hygroscopicus* (CPEP_SH; SP P11435), isocitrate lyase from *E. coli* (ICL_EC; SP P05313), 2-methylisocitrate lyase from *Salmonella typhimurium* (PRPB_ST; SP Q56062), hypothetical 33.1 kDa protein in the mmge-bfmbaa intergenic region from *B. subtilis* (YQIQ_BS; SP P54528), hypothetical 27.3 kDa protein CY39.20 from *M. tuberculosis* (YW20_MT; SP Q10859), unknown protein coding ORF3 in a gene cluster upstream from the *eryK* gene in *S. erythraea* (UNKN_ST; U82823), and hypothetical 34.2 kDa protein coding to a pSR132 cDNA clone in senescing Carnation flower petals in *D. caryophyllus* (UNKN_DC; PIR S35145). The programs used were ClustalW (*38*) from GCG (Wisconsin Genetics Computer Group) and SeqVu 1.0.1 from The Garvan Institute of Medical Research. The residues conserved among the four known PEP mutase sequences (*M. edulis*, *T. pyriformis* SP P33182, *S. hygroscopicus* SP P29247, and *S. wedmorensis* PIR S60206 PEP mutase sequences) are indicated in the figure by magenta coloring. The residues conserved among the 18 isocitrate lyase sequences found in the gene data bank are indicated in the figure by yellow coloring. Conserved residues among all eight of the aligned sequences are boxed, the *M. edulis* PEP mutase active site residues are numbered, and the sequence regions forming the mutase active site represented in Figure 1A are indicated by color-coded arrows.

Together, these observations suggest that the D58 to Ala replacement has eliminated catalysis without disrupting the native fold of the enzyme.

Conserved Residues within the PEP Mutase Superfamily. Protein homologues were identified using the PEP mutase sequences as queries in Advanced BLAST and PSI BLAST searches (*37*) of the NCBI data banks. The homologues include one CPEP mutase (*41*−*43*), two 2-methylisocitrate lyases (sharing >90% sequence identity) (*44*−*46*), eighteen isocitrate lyases (38−64% sequence identity among sequence pairs) (*47*), and several proteins of unknown function [viz., hypothetical 33.1 kDa protein in the mmge-bfmbaa intergenic region from *Bacillus subtilis* (Accession Number P54528), hypothetical 27.3 kDa protein CY39.20 from *Mycobacterium tuberculosis* (Accession Number Q10859), unknown protein coding ORF3 in a gene cluster upstream from the *eryK* gene in *Saccharopolyspora erythraea* (Accession Number U82823), and hypothetical 34.2 kDa protein coding to a pSR132 cDNA clone in senescing carnation flower petals in *Dianthus caryophyllus*] (*48*). Invariant positions (colored yellow in Figure 3) within the isocitrate lyase subfamily were identified by a ClustalW (*38*) generated alignment of the 18 sequences found in GenBank. A sequence comparison across the superfamily (one representative of each known protein function plus the four protein sequences having unknown function) is provided in Figure 3. Amino acid residues conserved in all eight sequences are boxed. The amino acid identities calculated for sequence pairs range from 25% to 40%.

DISCUSSION

PEP Mutase Model A Is Most Consistent with the Mutagenesis Data. Model B of Figure 2 predicts that R159 mediates the transfer of the PEP phosphoryl group from the C(2) oxygen to C(3) during catalytic turnover. Replacement of R159 with Ala reduces k_{cat} by 4 orders of magnitude but does not fully eliminate the catalytic activity. Thus, it is unlikely that R159 plays the pivotal role in catalysis required by model B. Model A of Figure 2 predicts that R159 binds to the carboxyl group of the PEP while D58 mediates the transfer of the substrate phosphoryl group. The decrease in activity observed for the R159A mutant is consistent with its proposed role in substrate anchoring and activation. Replacement of D58 with Ala eliminates catalytic turnover, the expected outcome for the replacement of the active site nucleophile with a nonnucleophilic residue such as Ala. The replacement of the other active site carboxylates, D85, D87, and E114, with Ala inhibits but does not eliminate catalysis. The K_m for Mg(II) activation (measured at saturating Ppyr) is, interestingly, 2-fold smaller for the D85A and D87A mutants than for the wild-type mutase, while that measured for the E114A mutant is ca. 8-fold larger. The multiple Mg(II) ligands apparantly compensate for the loss of a single ligand. The inhibited k_{cat} values observed for the D85A, D87A, and E114A mutants must result from the alteration of the steric and electronic environment within the Mg(II) binding site which, in turn, may lead to subtle changes in Mg(II) orientation and effective active site charge. In conclusion, model A is most consistent with the present structure and mutagenesis data. Efforts toward solving the crystal structure of the enzyme complexed with PEP and Mg(II) are in progress.

While model A is not incompatible with the dissociative pathway for PEP mutase catalysis (mechanism II, Scheme 2), the double-displacement pathway (mechanism I, Scheme 2) in which D58 functions in covalent catalysis has precedent among phosphoryl transfer enzymes (*25*−*28*). Our earlier attempts to detect the putative phosphoenzyme−pyruvate enolate intermediate using rapid-quench techniques failed (*19, 22*), suggesting that the energetics of the PEP mutase reaction are such that this intermediate does not accumulate to a detectable level during a single turnover. Presently, we are exploring ways to stabilize the intermediate through substrate and/or enzyme engineering so that its formation might be finally demonstrated.

Catalytic Motif of the PEP Mutase Superfamily. A comparison made between the PEP mutase structure (Figure 1A) and other α/β-barrel enzyme structures identified using the program DALI (*49*) suggests that the PEP mutase is representative of a α/β-barrel superfamily (CPEP mutase, isocitrate lyase, 2-methylisocitrate lyase, and several proteins of unknown function listed in Figure 3) not previously identified in the SCOP classification (*50*). Although the sequence divergence among the family members is modest, the chemistries represented are quite different. By comparing the sequences of the family members in the active site regions defined by the PEP mutase structure, we hoped to identify the common features of the catalytic machinery utilized by this group of enzymes.

As illustrated in Figure 1A, the PEP mutase catalytic residues are located on the C-terminal ends of barrel β-strands 2 (the oxyanion hole formed by residues 46−48 is shown in red; the sequence region 55−58 containing the putative active site nucleophile D58 is shown in blue), 3 [the sequence region 84−91 containing the Mg(II) binding residues D85 and D87 is shown in magenta], 4 [the sequence region 114−124 containing the Mg(II) binding residue E114 and PEP phosphoryl group binding residue K120 is shown in green], and 5 (the sequence region 158−162 containing the PEP carboxylate binding residue R159 is shown in orange). The stretches of sequence containing the PEP mutase catalytic residues are identified in the superfamily sequence alignment shown in Figure 3 using color-coded arrows. Inspection of Figure 3 reveals that the PEP mutase active site region is highly conserved within the superfamily. The Mg(II) binding residues D85 and E114 are invariant and D87 is selectively replaced by Glu, suggesting that the Mg(II) binding site observed in the PEP mutase structure exists in each of the superfamily members. Reports of Mg(II) activation of CPEP mutase (*41, 43*) and isocitrate lyase (*51, 52*) are consistent with this deduction (metal ion activation has not yet been tested in the other family members). The PEP mutase active site D58, proposed to transfer the PEP phosphoryl group, is invariant among the superfamily members, suggesting that it too has been recruited for catalytic function. R159, shown in model A of Figure 2 to function in PEP carboxylate binding in the mutase, also appears to be recruited for catalytic function within the superfamily. K120, the putative PEP phosphoryl binding residue, is found in most but not all of the family members.

So, how might an active site containing bound Mg(II), a base or nucleophile (D58), and two electrophiles (R159 and K120) be used to catalyze the intramolecular phosphoryl transfer and retro-aldol chemistry mediated by the two

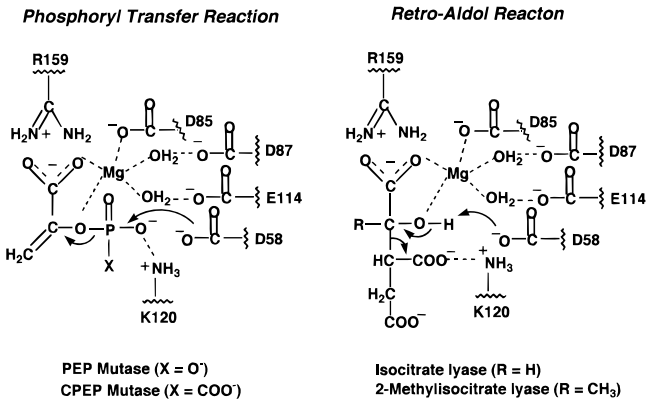

FIGURE 4: Hypothetical catalytic motif that supports the phosphoryl transfer reactions mediated by PEP mutase and CPEP mutase and the retro−aldol reactions mediated by isocitrate lyase and 2-methylisocitrate lyase.

mutases and the two lyases? In Figure 4, we propose a general catalytic motif that might account for the broad range of chemistry observed within the superfamily. Accordingly, D58 is suggested to transfer the substrate phosphoryl group in the mutase reactions and abstract the proton from the substrate hydroxyl group in the lyase reactions. The Mg(II) ion, on the other hand, may coordinate to the substrate oxygen atom undergoing bond cleavage as well as to the carboxyl substituent that is entering into conjugation as the bond cleavage proceeds. The R159 residue could also serve to anchor and activate the reaction center through interaction with the substrate carboxyl substituent. K120, which is available for interaction with the substrate phosphoryl group in the mutase reactions, might bind the carboxylate of the succinate unit in the lyase substrates.

While the models of mutase and lyase catalysis proposed in Figure 4 await evaluation within the context of family member structures [the X-ray crystal structure determination of isocitrate lyase is reportedly in progress (*53*)], hypothetical physiological ligands for the proteins having unknown function might be built on the basis of the common $^{-}O_2C-C-O-H(P)$ structural motif observed among the mutase and lyase substrates. In addition, the conservation of a Mg(II) binding site within these proteins is a strong indicator that Mg(II) is a required cofactor.

Conclusions. The present studies indicate that PEP mutase catalysis involves activation of the PEP pyruvate moiety through bidentate Mg(II) coordination of the carboxylate and C(2) O−P bridge oxygen atoms and by R159 ion pair formation with the carboxylate. The phosphoryl moiety, on the other hand, is activated for transfer by ion pair formation with K120 and H-bond formation with the backbone amide NHs of G46 and L48. The phosphoryl transfer itself is mediated by D58. The utilization of Mg(II) in conjunction with electropositive side chains to disperse electron density and an active site nucleophile to transfer the phosphoryl group is commonplace within the phosphotransferase enzyme sector, and thus, we might expect PEP mutase to belong to one of the many superfamilies of phosphoryl transfer enzymes. Instead, the active site arrangement conserved within the α/β fold links PEP mutase to an ancestor shared with the isocitrate lyases, enzymes specialized in C−C bond cleavage.

ACKNOWLEDGMENT

Mr. Lusong Luo and Mr. Alexander Kim are gratefully acknowledged for their assistance in preparing some of the figures reported in the manuscript.

REFERENCES

1. Horiguchi, M. (1972) *Biochim. Biophys. Acta 261*, 102−113.
2. Kuzuyama, T., Hidaka, T., Kamigiri, K., Imai, S., and Seto, H. (1992) *J. Antibiot. 45*, 1812−1814.
3. Hara, O., Murakami, T., Imai, S., Anzai, H., Itoh, R., Kumada, Y., Takano, E., Satoh, E., Satph, A., Nagaoka, K., and Thompson, C. (1991) *J. Gen. Microbiol. 137*, 351−359.
4. Ternan, N. G., McGrath, J. W., McMullan, G., and Quinn, J. P. (1998) *World J. Microbiol. Biotechnol. 14*, 635−647.
5. Hildebrand, R. L. (1983) *The Role of Phosphonates in Living Systems*, CRC Press, Inc., Boca Raton, FL.
6. Kennedy, K. E., and Thompson, G. A. (1970) *Science 168*, 989−991.
7. White, R. W., Kemp, P., and Dawson, R. M. C. (1970) *Biochem. J. 116*, 767−768.
8. Steiner, S., Conti, S. F., and Lester, R. L. (1973) *J. Bacteriol. 116*, 1199−1211.
9. Wassef, M. K., and Hendrix, J. W. (1977) *Biochim. Biophys. Acta 922*, 78−86.
10. Hakomori, S.-I. (1990) *J. Biol. Chem. 265*, 18713−18716.
11. Abe, S., Araki, S., Sataka, M., Fujiwara, N., Kon, K., and Ando, S. (1991) *J. Biol. Chem. 266*, 9939−9943.
12. Mastelerz, P. (1984) in *Natural Products Chemistry* (Zulewski, R. I., and Skolik, J. J., Eds.) p 171, Elsevier Science Publishers B. V., Amsterdam.
13. de Graaf, R. M., Visscher, J., and Schwartz, A. W. (1995) *Nature 378*, 474−477.
14. Hidaka, T., and Seto, H. (1989) *J. Am. Chem. Soc. 111*, 8012−8013.
15. Seidel, H. M., Pompliano, D., and Knowles, J. R. (1992) *Biochemistry 31*, 2598−2608.
16. Huang, K., Li, Z., Jia, Y., Dunaway-Mariano, D., and Herzberg, O. (1999) *Structure* (in press).
17. McQueney, M. S., Lee, S.-L., Swartz, W. H., Ammon, H. L., Mariano, P. S., and Dunaway-Mariano, D. (1991) *J. Org. Chem. 56*, 7121−7130.
18. Seidel, H. M., Freeman, S., Schwalbe, C. H., and Knowles, J. R. (1990) *J. Am. Chem. Soc. 112*, 8149−8155.
19. McQueney, M. S. (1991) Doctor of Philosophy Dissertation, University of Maryland, College Park, MD.
20. Seidel, H. M., and Knowles, J. R. (1994) *Biochemistry 33*, 5641−5646.
21. Kofron, J. L., and Reed, (1990) *Arch. Biochem. Biophys. 280*, 40−44.
22. Kim, J., and Dunaway-Mariano, D. (1996) *Biochemistry 35*, 4628−4635.
23. Buchbinder, J. H., and Reed, G. H. (1990) *Biochemistry 29*, 1799−1806.
24. Kofron, J. L., Ash, D. E., and Reed, G. H. (1988) *Biochemistry 27*, 4781−4787.
25. Webb, M. R., and Trentham, D. R. (1981) *J. Biol. Chem. 256*, 4884−4887.
26. Sanders, D. A., Gillece-Castro, B. L., Stock, A. M., Burlingame, A. L., and Koshland, D. E. (1989) *J. Biol. Chem. 264*, 21770−21778.
27. Collet, J. F., Stroobant, V., Pirard, M., Delpierre, G., and Van Schaftingen, E. (1998) *J. Biol. Chem. 273*, 14107−14112.
28. Baker, A. S., Ciocci, M. J., Metcalf, W. W., Kim, J.-B., Babbitt, P. C., Wanner, B. L., Martin, B. M., and Dunaway-Mariano, D. (1998) *Biochemistry 37*, 9305−9315.
29. Matte, A., Tari, L. W., and Delbaere, L. T. J. (1998) *Structure 6*, 413−419.
30. Sambrook, J., Fritsch, E. F., and Maniatis, T. (1989) *Molecular Cloning*, 2nd ed., Cold Spring Habor Press, Cold Spring Harbor, NY.
31. Erlich, H. A., Ed. (1992) *PCR Technology Principles and Applications for DNA Amplification*, W. H. Freeman and Co., New York.

32. Kim, A., Kim, J., Martin, B., and Dunaway-Mariano, D. (1998) *J. Biol. Chem. 273*, 4443−4448.
33. Sanger, F., Miklen, S., and Coulson, A. R. (1977) *Proc. Natl. Acad. Sci. U.S.A. 74*, 5463−5467.
34. Bowman, E., McQueney, M. S., Scholten, J. D., and Dunaway-Mariano, D. (1990) *Biochemistry 29*, 7059−7063.
35. Cleland, W. W. (1979) *Methods Enzymol. 63*, 103−138.
36. Bradford, M. (1976) *Anal. Biochem. 72*, 248−254.
37. Altschul, S. F., Madden, T. L., Schäffer, A. A., Zhang, J., Zhang, Z., Miller, W., and Lipman, D. J. (1997) *Nucleic Acids Res. 25*, 3389−3402.
38. Altschul, S. F., Gish, W., Miller, W., Myers, E. W., and Lipman, D. J. (1990) *J. Mol. Biol. 215*, 403−410.
39. Hidaka, T., Hidaka, M., and Seto, H. (1992) *J. Antibiot. 45*, 1977−1980.
40. Hidaka, T., Goda, M., Kuzuyama, T., Takei, N., Hidaka, M., and Seto, H. (1995) *Mol. Gen. Genet. 249*, 274−280.
41. Hidaka, T., Imai, S., Hara, O., Anzai, H., Murakami, T., Nagaoka, K., and Seto, H. (1990) *J. Bacteriol. 172*, 3066−3072.
42. Hidaka, T., Hidaka, M., Uozumi, T., and Seto, H. (1992) *Mol. Gen. Genet. 233*, 476−478.
43. Pollack, S. J., Freeman, S., Pompliano, D. L., and Knowles, J. R. (1992) *Eur. J. Biochem. 209*, 735−743.
44. Horswill, A. R., and Escalante-Semerena, J. C. (1997) *J. Bacteriol. 179*, 928−940.
45. Tsang, A. W., Horswill, A. R., and Escalante-Semerena, J. C. (1998) *J. Bacteriol. 180*, 6511−6518.
46. Blattner, F. R., Plunkett, G., III, Bloch, C. A., Perna, N. T., Burland, V., Riley, M., Collado-Vides, J., Glasner, J. D., Rode, C. K., Mayhew, G. F., Gregor, J., Davis, N. W., Kirkpatrick, H. A., Goeden, M. A., Rose, D. J., Mau, B., and Shao, Y. (1997) *Science 277*, 1453−1474.
47. Rieul, C., Bleicher, F., Duclos, B., Cortay, J. C., and Cozzone, A. J. (1988) *Nucleic Acids Res. 16*, 5689.
48. Wang, H., Brandt, A. S., and Woodson, W. R. (1993) *Plant Mol. Biol. 22*, 719−724.
49. Holm, L., and Sander, C. (1993) *J. Mol. Biol. 233*, 123−138.
50. Murzin, A. G., Brenner, S. E., Hubbard, T., and Chothia, C. (1995) *J. Mol. Biol. 247*, 536−540.
51. Giachetti, E., Pinzauti, G., Bonaccorsi, R., and Vanni, P. (1988) *Eur. J. Biochem. 172*, 85−91.
52. Giachetti, E., and Vanni, P. (1991) *Biochem. J. 276*, 223−230.
53. Langridge, S. J., Baker, P. J., Delucas, J. R., Sedelnikova, S. E., Turner, G., and Rice, D. W. (1997) *Acta Crystallogr., Sect. D, Biol. Crystallogr. 53*, 488−490.
54. Kraulis, P. J. (1991) *J. Appl. Crystallogr. 24*, 946−950.

BI990771J